Further explorations of Skyrme-Hartree-Fock-Bogoliubov mass formulas. VII. Simultaneous fits to masses and fission barriers

S. Goriely,[1,*] M. Samyn,[1] and J. M. Pearson[2]
[1]*Institut d'Astronomie et d'Astrophysique, ULB-CP226, 1050 Brussels, Belgium*
[2]*Déparetment de Physique, Université de Montréal, Montréal (Québec), H3C 3J7, Canada*
(Received 20 December 2006; revised manuscript received 27 March 2007; published 19 June 2007)

We present a new Hartree-Fock-Bogoliubov mass model, HFB-14, that is fitted to the fission data through adjustment of a vibrational term in the phenomenological collective correction. The rms deviation of the model from the 2149 measured masses of nuclei with $Z, N \geqslant 8$ is 0.729 MeV. The rms deviation for all 77 primary barriers listed in the RIPL-2 data compilation is 1.31 MeV, and only 0.67 MeV for the 52 primary barriers of nuclei lower than 9 MeV, the ones of greater astrophysical interest. A similar accuracy is obtained (0.65 MeV) for the 45 secondary experimental barriers necessary for a reliable calculation of fission probabilities.

DOI: 10.1103/PhysRevC.75.064312 PACS number(s): 21.30.Fe, 21.10.Dr, 21.60.−n, 24.75.+i

I. INTRODUCTION

The r-process of stellar nucleosynthesis is known to depend on the masses and fission barriers (among other quantities) of nuclei that are so neutron rich that there is no hope of being able to measure them in the laboratory in the foreseeable future. It is thus of the greatest importance to be able to make reliable extrapolations of these quantities away from the known region, relatively close to the stability line, out toward the neutron drip line. To put these extrapolations on as rigorous a footing as is feasible at the present time, we have constructed a series of mass models based on the Hartree-Fock-Bogoliubov (HFB) method with Skyrme forces and a δ-function pairing force.

Of all our mass models, it is model HFB-8 (for which the corresponding set of force parameters is labeled BSk8) [1] that gives the best fit to the mass data: for the 2149 measured nuclei with $Z, N \geqslant 8$ [2], the rms error is 0.635 MeV. Using this force, we then calculated most of the measured fission barriers of nuclei with $Z \geqslant 80$ [3]. For nuclei with $Z \geqslant 92$ the rms deviation of the calculated heights of the primary barriers from the experimental values was only 0.72 MeV, but the results were much poorer for the primary barriers of nuclei with $Z < 92$: they were never less than 1.1 MeV too high and could be as much as 5.7 MeV too high, a much worse performance than that of the ETFSI method [4]. The sudden deterioration in the HFB primary barriers of Ref. [3] as we pass from $Z = 92$ to $Z = 91$ was found to be correlated with a rapidly growing third barrier lying at very large deformation. Clearly, fitting a model to nuclear masses does not explore all the regions of deformation space that are relevant to barriers, from which it follows that a good mass fit will not necessarily guarantee good barriers. In this note we show that it is possible, through adjustment of a phenomenological vibrational term that we have included for the first time in our model, to obtain drastically improved barriers without any deterioration of the mass fit.

Since the publication of the HFB-8 mass model we have generated several new mass models, but the direction of our work has shifted. Rather than seek ever better fits to the mass data our concern has been more with the construction of a *universal* force for all the various astrophysical applications, and to this end we have been imposing on our mass models extra constraints. Our latest published model [5], HFB-13 (force BSk13), was subjected to the two following constraints: (i) The energy-density curve of neutron matter was fitted, a requirement that is relevant not only to neutron-star applications but also to the reliability of finite-nucleus extrapolations out toward the neutron drip line. (Actually, the HFB-8 model was itself subjected to a weak constraint, namely the requirement that neutron matter not collapse at subnuclear densities. Without this constraint a still better fit to the mass data could have been obtained, but there would have been a contradiction with the undisputed existence of neutron stars.) (ii) The pairing force was considerably weakened with respect to that of all our previously published mass models, for which the pairing was excessively strong, in the sense that despite their good mass fits the calculated spectral pairing gap was much bigger than the experimental even-odd mass differences. Even if this excessively strong pairing had not impaired the mass fits—indeed, it had arisen automatically in the process of optimizing the mass fit—it was believed to be at least partially responsible for the unsatisfactory results found in the fission-barrier calculations of Ref. [3] and in the level-density calculations of Ref. [6] (another nuclear quantity of astrophysical importance).

Despite the imposition of these two conditions, the quality of the mass fit was only slightly worse with HFB-13 than with HFB-8, the rms deviation rising to an acceptable 0.717 MeV for the same data set. That the deterioration was not worse might be due to our adoption of the Bulgac-Yu procedure [7] for regularizing the pairing force, *with the additional feature of a low cutoff*.

Already it has been shown that the reduced pairing strength of force BSk13 leads to the expected improvement in level densities [8], and we turn now to the question of the fission barriers. Unfortunately, we cannot use the force BSk13 as the starting point, because we used there the value of $0.92M$ for the isoscalar effective mass M_s^* at the equilibrium density ρ_0 of symmetric infinite nuclear matter, this being the value found

*sgoriely@astro.ulb.ac.be

by Zuo *et al*. from extended Brueckner-HF calculations using realistic nucleon-nucleon forces [9]. Very recently, after the publication of Refs. [5,8], it was learned that this value of M_s^* must be drastically modified when three-nucleon forces are taken into account, a value of $0.825M$ at the density ρ_0 now being found [10]. This lower value is also favored by measurements of the giant quadrupole resonance [11,12]. Thus we must first construct a new mass model that takes account of this reduction in the value of M_s^*, while maintaining the neutron-matter and pairing constraints of the HFB-13 model.

In Sec. II we present this new model, labeled HFB-14.0 (force BSk14), whereas in Sec. III we describe our fission-barrier calculations with this model. Our results in this respect are far from satisfactory, in large part because of the behavior of the collective correction at large deformations (see especially Sec. III of Ref. [1]). We show in Sec. IV that with an appropriate modification of this correction the same BSk14 force leads to drastically improved barriers with only a minimal impact on the quality of the mass fit. This new correction, along with the force BSk14, defines model HFB-14.

II. THE HFB-14.0 MODEL

We calculate masses in essentially the same way as for the HFB-13 model [5], retaining in particular the neutron-matter and pairing constraints, but reducing M_s^* to $0.8M$. The only other difference is that we now make provision for subtracting a much more general form of collective correction from the calculated masses,

$$E_{\rm coll} = E_{\rm rot}^{\rm crank}\left\{b\tanh(c|\beta_2|) + d\exp\left[-l\left(\beta_2-\beta_2^0\right)^2\right]\right\}, \quad (1)$$

in which $E_{\rm rot}^{\rm crank}$ denotes the cranking-model value of the rotational correction and β_2 the quadrupole deformation, whereas all other parameters are phenomenological. In the actual mass fit, labeled model HFB-14.0, we drop the second term here, leaving just the rotational correction that we have always made (the role of the second term will be to fit to fission barriers, without any further change in the force determined by the mass fit, determining thereby model HFB-14). The set of force parameters for the Skyrme, pairing, and Wigner components resulting from the mass fit is labeled BSk14 and is shown in Table I. The only exceptional feature in this table is the very small value of t_2 and the very large value of x_2, signifying that the ^1P and ^3P interactions have strengths of comparable magnitude but opposite signs, the former being repulsive. As far as the signs of these two states are concerned there is no change here from the force BSk13, but the ^1P repulsion is now much stronger than before [5]. The values of the parameters b and c emerging from the mass fit are shown in the first column of Table II. Despite the change in M_s^*, the rms deviation given by the model HFB-14.0 for the same data set of 2149 measured nuclei is virtually the same as for HFB-13: $\sigma = 0.716$ MeV (mean deviation $\bar{\epsilon} = 0.02$ MeV).

Table III shows the parameters of infinite (INM) and semi-infinite (SINM) nuclear matter for the force BSk14, defined as in Ref. [5]. These parameters are independent of the collective correction and thus hold equally well for models HFB-14.0 and HFB-14.

TABLE I. Parameter set BSk14 (for mass models HFB-14.0 and HFB-14).

t_0 (MeV fm^3)	−1822.67
t_1 (MeV fm^5)	377.470
t_2 (MeV fm^5)	−2.41056
t_3 (MeV fm$^{3+3\gamma}$)	11406.3
x_0	0.302096
x_1	−0.823575
x_2	61.9411
x_3	0.473460
W_0 (MeV fm^5)	135.565
γ	0.3
V_n^+ (MeV fm^3)	−240.0
V_n^- (MeV fm^3)	−265.5
V_p^+ (MeV fm^3)	−252.4
V_p^- (MeV fm^3)	−261.5
ε_Λ (MeV)	7.0
V_W (MeV)	−1.70
λ	400.0
V'_W (MeV)	0.75
A_0	30.0

TABLE II. Parameters of collective correction for models HFB-14.0 and HFB-14.

	HFB-14.0	HFB-14
b (MeV)	1.25	0.8
c	8.0	8.0
d (MeV)	0.0	0.4
l	–	6.0
β_2^0	–	0.3

TABLE III. Macroscopic parameters for force BSk14 (mass models HFB-14.0 and HFB-14). The first 12 lines refer to infinite nuclear matter, the last 2 to semi-infinite nuclear matter.

a_v (MeV)	−15.853
ρ_0 (fm^{-3})	0.1586
J (MeV)	30.0
M_s^*/M	0.80
M_v^*/M	0.78
K_v (MeV)	239.3
L (MeV)	43.91
G_0	−0.63
G'_0	0.51
G_1	1.49
G'_1	0.44
$\rho_{\rm frmg}/\rho_0$	1.24
a_{sf} (MeV)	17.6
Q (MeV)	35.0

TABLE IV. Fission barriers and isomeric states: rms (σ) and mean ($\bar{\epsilon}$) deviations (in MeV) between data and predictions for models HFB-14.0 and HFB-14. The numbers in parentheses correspond to the number of cases.

		HFB-14.0		HFB-14	
		σ	$\bar{\epsilon}$	σ	$\bar{\epsilon}$
$80 \leqslant Z \leqslant 96$	Primary (77)	1.61	1.05	1.31	−0.72
–	Secondary (45)	2.00	1.87	0.65	0.17
–	Isomers (30)	2.22	2.17	0.76	0.63
$88 \leqslant Z \leqslant 96$	Primary (52)	1.22	0.80	0.67	−0.36

The energy-density curve of neutron matter for force BSk14, corresponding to $J = 30$ MeV, is indistinguishable from the realistic [13] curve up to the supernuclear density of 0.2 neutrons per fm^3, as are all our other forces (BSk9 to 13) that have been fitted to $J = 30$ MeV (see Fig. 13 of Ref. [5]). Slight differences do emerge for higher densities, but this is a domain in which there is no reason to expect Skyrme forces to be valid anyway.

III. FISSION BARRIERS IN THE HFB-14.0 MODEL

The constrained HFB calculations that we report here were performed in essentially the same way as with the barrier calculations for the model HFB-8 [3], with the following important difference: whereas before we constrained the HFB calculations to different given values of the quadrupole, octupole, and hexadecapole moments, Q_2, Q_3, and Q_4, respectively, we now follow the usual practice (see, for example, Refs. [14,15]) of constraining only Q_2, making, for different fixed values of Q_{2c}, an unrestricted variation of the modified energy

$$\bar{E} = E + \tfrac{1}{2} c_q (Q_2 - Q_{2c})^2, \tag{2}$$

where $E = \langle H \rangle$, the expectation value of the unconstrained model Hamiltonian H, and c_q is a somewhat arbitrary strength constant. Thus for each value of Q_{2c} we will be implicitly minimizing with respect to Q_3 and Q_4 (and all other multipoles) rather than holding them at fixed values. It turns out that the converged value of Q_2 always lies very close to its target value Q_{2c}, much closer than can sometimes be the case when other constraints are applied at the same time. We believe that this procedure is safer than the one we followed earlier [3], and we stress that the way in which we compute the fission path in the (Q_2, Q_3, Q_4) hyperplane ensures that there can be no discontinuities of the fission path, i.e., no unseen flips from one hypervalley to another [3,16]. However, there may be the occasional possibility of branching up the wrong valley. For example, when confronted with a choice between two valleys our procedure will choose the more gently climbing one, which later, however, might start to climb more steeply and lead to a higher saddle point than the other valley might have done. This implies that our calculated barriers could be higher, but never lower, than the true barriers corresponding to the given force.

We calculate barriers for all the 77 nuclei for which barrier data are given in the RIPL-2 compilation [17]. The deviations (experiment-theory) for model HFB-14.0 are displayed in Fig. 1, the upper panel showing the 77 primary barriers that have been measured, the middle panel the 45 secondary barriers, and the lower panel the 30 isomeric states (the data for these come from Table I of Ref. [1]). The rms and mean values of these deviations are shown in the first and second columns, respectively, of Table IV. The first three lines refer to the complete RIPL-2 data set of 77 nuclei, for which $80 \leqslant Z \leqslant 96$: the first line corresponds to the primary barriers, the second to the secondary barriers, and the third to isomeric states. It will be seen from Fig. 1 that the errors tend to be larger for the lighter nuclei. What does not appear on this figure is that the barriers themselves tend to be much higher for the lighter nuclei. In fact, the data we have used fall into two distinct groups: for $Z \geqslant 88$ no barrier is higher than 8.5 MeV,

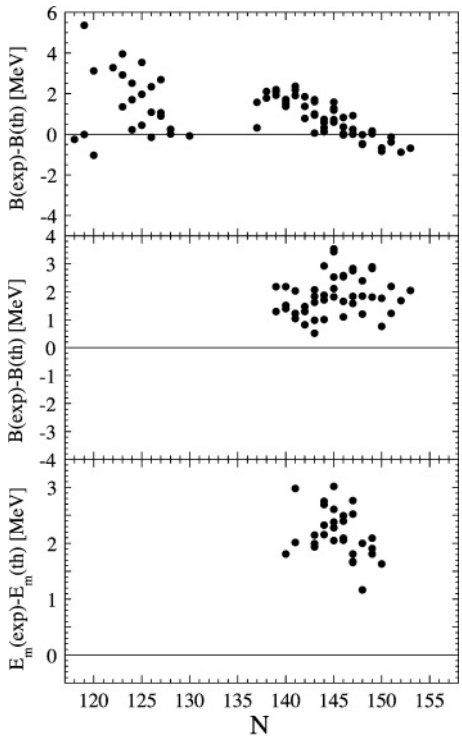

FIG. 1. Deviations between model HFB-14.0 and experiment for (a) upper panel: primary barriers; (b) middle panel: secondary barriers; (c) lower panel: isomeric states.

TABLE V. Rms (σ) and mean ($\bar{\epsilon}$) deviations between data and predictions for model HFB-14; for convenience we also show models HFB-8 [1], HFB-13 [5], FRDM [18], and FRLDM [18]. The first pair of lines refers to all the 2149 measured masses M, the second pair to the masses M_{nr} of the subset of 185 neutron-rich nuclei with $S_n \leqslant 5.0$ MeV, and the third pair to charge radii (782 measured values). The last line shows the calculated neutron-skin thickness of ^{208}Pb for these forces.

	HFB-14	HFB-8	HFB-13	FRDM	FRLDM
$\sigma(M)$ (MeV)	0.729	0.635	0.717	0.656	0.769
$\bar{\epsilon}(M)$ (MeV)	−0.057	0.009	−0.039	0.058	−0.403
$\sigma(M_{nr})$ (MeV)	0.833	0.838	0.813	0.910	0.955
$\bar{\epsilon}(M_{nr})$ (MeV)	0.261	−0.025	0.257	0.047	−0.078
$\sigma(R_c)$ (fm)	0.0309	0.0275	0.0296	0.0545	0.159
$\bar{\epsilon}(R_c)$ (fm)	−0.0117	0.0025	−0.0099	−0.0366	−0.151
$\theta(^{208}\text{Pb})$ (fm)	0.16	0.12	0.16	–	–

whereas for $Z < 88$ no barrier is lower than 13.5 MeV. Now barriers as high as those of the second group play no active role in astrophysics, and it is less necessary to have precise knowledge of their heights. Accordingly, in the last line we show the deviations for the primary barriers of the subset of 52 nuclei with $Z \geqslant 88$ (all the secondary barriers and isomers fall into this subset, and their deviations will be as given in the two preceding lines). We see that the results are somewhat better for this important subset, but the secondary barriers as well as the isomeric states remain systematically and unacceptably too low. The overall accuracy is not sufficient to inspire confidence in the use of this model for calculating barriers of nuclei in the far neutron-rich region.

IV. THE HFB-14 MODEL

An inspection of the barriers calculated in the HFB-14.0 model shows that the problem can be attributed to its purely rotational collective correction of Eq. (1) being too high at the large deformations relevant to barriers. (This can be seen from the middle panel of Fig. 1 for secondary barriers, most of which are outer barriers.) So far we have made no attempt to include explicitly a vibrational correction, but rather have simply absorbed any such neglected effect into the mass fit of the force. That the precision of our mass fits has been so good simply reflects the fact that vibrational effects contribute to all nuclei, and in particular to spherical nuclei. However, it is too much to expect that the renormalization of the force that we have implicitly made in the mass fit will continue to represent correctly vibrational effects at deformations larger than those encountered in ground states. To correct for this missing part of the vibrational correction we activate the second term in Eq. (1), our final choice for the parameters being given in the second column of Table II; note particularly that b has changed from its original value for model HFB-14.0. The physical meaning of the new collective correction will be discussed in more detail below.

We find that with this new collective correction the force BSk14 that was determined once and for all in the mass fit HFB-14.0, i.e., with the purely rotational collective correction, gives much improved barriers, with the mass fit being only slightly affected, the rms deviation rising from 0.716 to 0.729 MeV. This defines our model HFB-14, and we now comment in more detail on its predictions for masses and barriers.

A. Masses

The rms and mean (data-theory) values of the deviations between the usual data set of 2149 measured nuclear masses and the HFB-14 predictions are given in the first and second lines, respectively, of Table V, where we also compare with our "best-fit" model HFB-8 [1], with HFB-13, with the FRDM (finite-range droplet model) [18], and with the FRLDM (finite-range liquid-droplet) model [18]. It will be seen that as far as the agreement with the complete set of mass data is concerned, we continue with this new model to lose the advantage over the FRDM that we held with HFB-8. However, of crucial importance for extrapolating to the unknown neutron-rich region is the performance of the model in question for the most neutron-rich measured nuclei. Accordingly, in the next pair of lines we show the rms and mean deviations for the subset of the mass data consisting of the 185 neutron-rich nuclei having a neutron-separation energy $S_n \leqslant 5.0$ MeV. In this respect the HFB-Skyrme models continue, with HFB-14, to perform better than the FRDM. As for the FRLDM, which is now preferred to the FRDM for barrier calculations [16], its mass fits are unequivocally inferior to those of our present model.

For completeness we also show in Table V the rms and mean deviations between the theoretical and experimental rms charge radii for the 782 nuclei with $Z, N \geqslant 8$ listed in the 2004 compilation [19] (lines 5 and 6, respectively). The excellent agreement with experiment for a physical quantity that was not included in the fitting of the force is a test (necessary, but by no means sufficient) of the underlying soundness of our HFB mass models. The last line shows the model value for ^{208}Pb of the neutron-skin thickness $\theta \equiv R_n^{\text{rms}} - R_p^{\text{rms}}$, where R_n^{rms} is the rms radius of the neutron distribution and R_p^{rms} that of the point-proton distribution. Within the framework of conventional Skyrme forces θ appears to be rigorously determined by the value of the symmetry

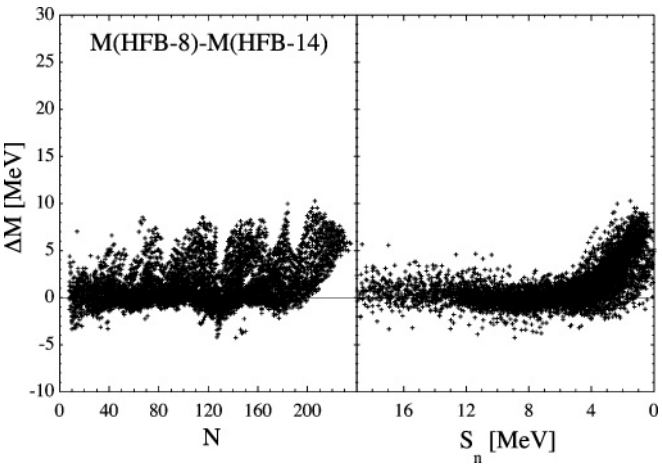

FIG. 2. Differences between model HFB-8 and HFB-14 mass predictions as a function of (left) N and (right) S_n.

coefficient J. Experimentally, θ is not very well determined in a model-independent way, but the forthcoming Jefferson experiment using parity-violating electron scattering [20,21] should improve the situation considerably in this respect. However, the expected accuracy of ± 0.05 fm will not tie down J to better than ± 2 MeV.

We have constructed for model HFB-14 a complete mass table going from one drip line to the other over the range Z and $N \geqslant 8$ and $Z \leqslant 110$. In Figs. 2 and 3 we compare these predictions with those of our "best-fit" model HFB-8 and with those of the FRDM, respectively, plotting the differences as a function of both the neutron number N and the neutron-separation energy S_n. In both cases we see that despite the close similarity in the quality of the fits to the data given by these different models, large differences emerge as the neutron-drip line is approached, although the divergence is much larger in the latter case (a large part of the divergence between HFB-8 and HFB-14 can be attributed to the imposition of the neutron-matter constraint in the latter but not the former).

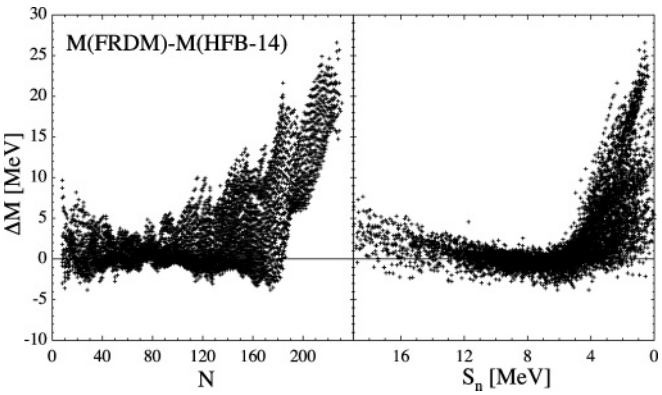

FIG. 3. Differences between the FRDM and HFB-14 mass predictions as a function of (left) N and (right) S_n.

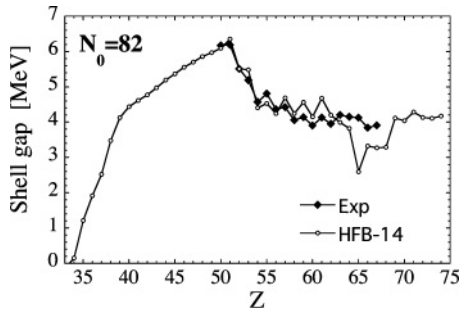

FIG. 4. $N_0 = 82$ shell gap as function of Z for mass model HFB-14.

1. Neutron-shell gaps

We have calculated the neutron-shell gaps, defined by

$$\Delta_n(N_0, Z) = S_{2n}(N_0, Z) - S_{2n}(N_0 + 2, Z), \qquad (3)$$

as a function of Z for the magic numbers $N_0 = 50, 82, 126$, and 184, respectively, for the model HFB-14. The shell gaps are qualitatively similar to the ones obtained previously with our HFB models. The major change of interest is in Fig. 4 for the $N_0 = 82$ shell gap, where the predicted shell gap is seen to be in excellent agreement with experiment: it is particularly to be noted that this is the first of our HFB models to correctly reproduce the enhancement associated with the double magicity at $Z = 50$, i.e., for ^{132}Sn. Consequently, the shell gap remains much higher when going down the $N_0 = 82$ isotone chain toward lower proton numbers, remaining above 4 MeV even for ^{122}Zr; a strong shell quenching appears only for lighter elements. However, we still do not correctly reproduce the double magicity in the vicinity of ^{208}Pb.

B. Barriers

Figure 5 and the last two columns of Table IV show that model HFB-14 has led to a significant improvement over model HFB-14.0. In particular, the rms deviation for the 52 primary barriers of nuclei with $88 \leqslant Z \leqslant 96$, which are always less than 9 MeV high, is as low as 0.67 MeV. A similar accuracy is obtained (0.65 MeV) for the secondary barriers, good values for which are necessary for a reliable calculation of fission probabilities. Model HFB-14 definitely outperforms the ETFSI model [4] and is well suited for a new calculation of all the barriers involved in the r-process. Such an extrapolation from the measured barriers, when it becomes available, will have to be considered as more reliable than the similar compilation made with the ETFSI model [22]. As a first result of the new compilation, we find for the primary barrier of the crucial semimagic ($N = 184$) nucleus ^{276}U a height of 13.2 MeV, which is to be compared with the value of 17.7 MeV found with the ETFSI method [22].

C. Comments on the collective correction of model HFB-14

We show in Fig. 6 the collective correction $E_{\rm coll}$ in ^{240}Pu for the two models HFB-14.0 and HFB-14 as a function of

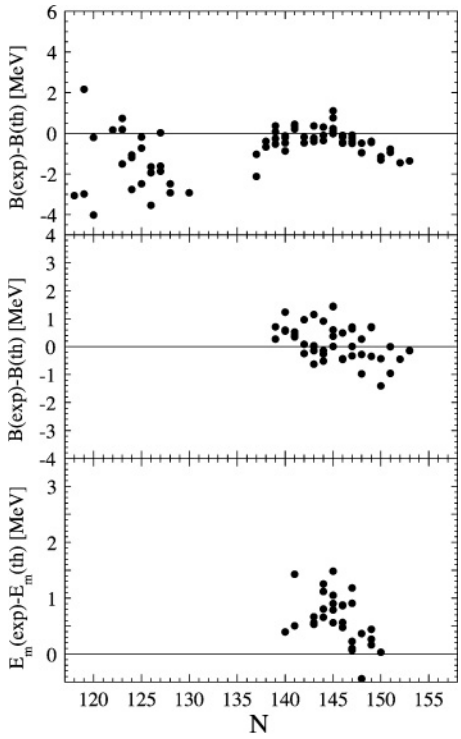

FIG. 5. Deviations between model HFB-14 and experiment for (a) upper panel: primary barriers; (b) middle panel: secondary barriers; (c) lower panel: isomeric states.

the quadrupole deformation β_2. The required reduction of the HFB-14.0 correction at large deformations, realized in Eq. (1) for model HFB-14, will be seen. Our confidence in this latter model as a tool for extrapolation will be enhanced if we can acquire some understanding of the physical origin of the collective correction of Eq. (1), especially the second term: the improvement over the barriers of model HFB-14.0 brought about by model HFB-14 is entirely a result of the three extra fitting parameters provided by this term.

Concerning the first term of Eq. (1), we recall that it is intended to represent the rotational correction, the cranking-model value of which is given by

$$E_{\rm rot}^{\rm crank} = \frac{\langle MF|\hat{J}^2|MF\rangle}{2\mathcal{I}^{\rm crank}}, \tag{4}$$

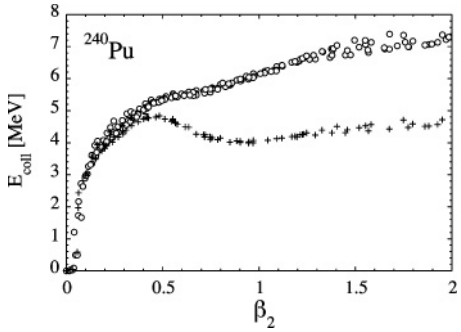

FIG. 6. Collective corrections for models HFB-14.0 (upper curve) and HFB-14 (lower curve).

where $|MF\rangle$ denotes the mean-field state, $\hat{J}$ is the total angular momentum operator in the intrinsic frame, and $\mathcal{I}^{\rm crank}$ the moment of inertia in the cranking model. Then taking into account the normalization factor b, we can write

$$b\,E_{\rm rot}^{\rm crank} = \frac{\langle MF|\hat{J}^2|MF\rangle}{2\mathcal{I}'}, \tag{5}$$

where $\mathcal{I}' = \mathcal{I}^{\rm crank}/b$. It turns out that with the value $b = 0.8$ found for model HFB-14 the values of $\mathcal{I}'$ are consistent with the experimental values of the moment of inertia (see Table 1 of Ref. [23] for a compilation of the latter values). This value of b is also in agreement with the value of 0.75 obtained in Ref. [24] for the dynamical correction to the standard Inglis-Belyaev expression, this value being shown in addition to remain almost deformation-independent. This suggests that the first term of Eq. (1) is indeed representing a rotational correction. On the other hand the value of $b = 1.25$ found in model HFB-14.0 is quite inconsistent with the experimental values of the moment of inertia, which suggests that the fit was in some way attempting (not altogether successfully) to simulate the missing second term.

With the first term of Eq. (1) thus being identified with a rotational correction $E_{\rm rot}$, it is tempting to regard the second term as representing a vibrational correction, or rather quasi-vibrational correction $E_{\text{“vib”}}$, in the sense that it only has to correct for the high-deformation part of the real vibrational correction that is not absorbed into the Skyrme part of the interaction BSk14 by the mass fit. This interpretation is strengthened by the microscopic calculations of Ref. [25], where it is shown that the vibrational correction decreases with increasing deformation (see Fig. 16 of that article).

It should be stressed that although we allow for left-right asymmetry in our model, we take no account of triaxiality. Because this is probably not a phenomenon that is sufficiently widespread to influence the force through the mass fit, its role in fission will be absorbed by the collective correction, the major share being taken by $E_{\text{“vib”}}$ if $E_{\rm rot}$ is truly a rotational term. The $E_{\text{“vib”}}$ term will likewise have to absorb other neglected effects, such as a possible dependence of the pairing strength on deformation (through a surface dependence).

V. CONCLUSIONS

We have presented a new mass model, HFB-14, that has the following advantages over our “best mass-fit” model HFB-8: (a) it fits neutron matter, (b) it has minimal pairing strength, and (c) it gives significantly improved fission barriers (better than those given by both the ETFSI method [4] and the model HFB-8 [3]). Despite these extra physical constraints and the requirement of much better barriers, the rms deviation of the mass fit is only slightly worse than that of HFB-8: 0.729 rather than 0.635 MeV. This slight loss in quality of the mass fit is well worth the much greater applicability of the model to astrophysical problems. In particular, we believe that no other mean-field model fits both masses and barriers so well.

A key element in the improvement of the barriers is the use of a more elaborate collective correction, simulating

both rotational and vibrational effects. This device has made possible a decoupling of the mass fit from the fit to barriers, thereby avoiding the computationally daunting task of refitting the force parameters to both masses and barriers. It is important to realize that this success has been achieved without resort to a deformation-dependent Wigner term, of the type used in Ref. [16]; as discussed in Sec. II of Ref. [3] the independent evidence points against the existence of such a term.

It is to be hoped that ultimately a deeper understanding of the collective correction used here will become available in terms of a complete microscopic treatment of vibrations and a thorough analysis of triaxiality (including a simultaneous left-right asymmetry). Even though such a program presents a serious challenge, it will have to be realized if one is to claim that one has a complete understanding of fission. In the meantime, however, we believe that with HFB-14 it is already possible to reliably calculate with the same model both the masses and the fission barriers of the experimentally inaccessible nuclei that are involved in the r-process of nucleosynthesis.

ACKNOWLEDGMENTS

S. G. thanks the FNRS (Belgium) and J. M. P. the NSERC (Canada) for financial support.

[1] M. Samyn, S. Goriely, M. Bender, and J. M. Pearson, Phys. Rev. C **70**, 044309 (2004).
[2] G. Audi, A. H. Wapstra, and C. Thibault, Nucl. Phys. **A729**, 337 (2003).
[3] M. Samyn, S. Goriely, and J. M. Pearson, Phys. Rev. C **72**, 044316 (2005).
[4] A. Mamdouh, J. M. Pearson, M. Rayet, and F. Tondeur, Nucl. Phys. **A644**, 389 (1998).
[5] S. Goriely, M. Samyn, and J. M. Pearson, Nucl. Phys. **A773**, 279 (2006).
[6] P. Demetriou and S. Goriely, Nucl. Phys. **A695**, 95 (2001).
[7] A. Bulgac and Y. Yu, Phys. Rev. Lett. **88**, 042504 (2002).
[8] S. Hilaire and S. Goriely, Nucl. Phys. **A779**, 63 (2006).
[9] W. Zuo, I. Bombaci, and U. Lombardo, Phys. Rev. C **60**, 024605 (1999).
[10] L. G. Cao, U. Lombardo, C. W. Shen, and N. V. Giai, Phys. Rev. C **73**, 014313 (2006).
[11] O. Bohigas, A. M. Lane, and J. Martorell, Phys. Rep. **51**, 267 (1979).
[12] S. Goriely, M. Samyn, J. M. Pearson, and E. Khan, Eur. Phys. J. A **25**, 71 (2005).
[13] B. Friedman and V. R. Pandharipande, Nucl. Phys. **A361**, 502 (1981).
[14] H. Flocard, P. Quentin, A. K. Kerman, and D. Vautherin, Nucl. Phys. **A203**, 433 (1973).
[15] A. Staszczak, J. Dobaczewski, and W. Nazarewicz, Int. J. Mod. Phys. E **15**, 302 (2006).
[16] P. Möller, A. J. Sierk, and A. Iwamoto, Phys. Rev. Lett. **92**, 072501 (2004).
[17] *Handbook for Calculations of Nuclear Reaction Data, RIPL-2*, IAEA-TECDOC-1506 (2006); www-nds.iaea.org/RIPL-2/
[18] P. Möller, J. R. Nix, W. D. Myers, and W. J. Swiatecki, At. Data Nucl. Data Tables **59**, 185 (1995).
[19] I. Angeli, At. Data Nucl. Data Tables **87**, 185 (2004).
[20] C. J. Horowitz, S. J. Pollock, P. A. Souder, and R. Michaels, Phys. Rev. C **63**, 025501 (2001).
[21] R. Michaels, http://hallaweb.jlab.org/parity/prex.
[22] A. Mamdouh, J. M. Pearson, M. Rayet, and F. Tondeur, Nucl. Phys. **A679**, 337 (2001).
[23] J. M. Pearson, Y. Aboussir, A. K. Dutta, R. C. Nayak, M. Farine, and F. Tondeur, Nucl. Phys. **A528**, 1 (1991).
[24] J. Libert, M. Girod, and J.-P. Delaroche, Phys. Rev. C **60**, 054301 (1999).
[25] P.-G. Reinhard, D. J. Dean, W. Nazarewicz, J. Dobaczewski, J. A. Maruhn, and M. R. Strayer, Phys. Rev. C **60**, 014316 (1999).